CONF-9510109--5

DOE/MC/29061-96/C0658

Lean Premixed Flames for Low NO_x Combustors

Author:

P. Sojka
L. Tseng
J. Bryjak
J. Gore
Y. Sivathanu
A. Kelkar
C. Rama
N. Laurendeau
M. Klassen
D. Thomsen

Contractor:

South Carolina Energy Research and Development Center
Clemson University
Clemson, SC 29634

Contract Number:

DE-FC21-92MC29061
Purdue University Subcontract No. 93-01-SR009

Conference Title:

Advanced Turbine Systems Annual Program Review

Conference Location:

Morgantown, West Virginia

Conference Dates:

October 17-19, 1995

Conference Sponsor:

U.S. Department of Energy, Office of Power Systems Technology,
Morgantown Energy Technology Center

Contracting Officer Representative (COR):

Norman Holcombe

Disclaimer

P3 Lean Premixed Flames for Low NO_x Combustors

P. Sojka, L. Tseng, J. Bryjak (sojka@ecn.purdue.edu; 317-494-1536)
J. Gore, Y. Sivathanu, A. Kelkar, C. Rama (gore@ecn.purdue.edu; 317-494-1452)
N. Laurendeau, M. Klassen, D. Thomsen (laurende@ecn.purdue.edu; 317-494-2713)
Thermal Sciences and Propulsion Center
School of Mechanical Engineering
Purdue University
West Lafayette, IN 47907

Introduction

Gas turbines are being used throughout the world to generate electricity. Due to increasing fuel costs and environmental concerns, gas turbines must meet stringent performance requirements, demonstrating high thermal efficiencies and low pollutant emissions. In order for U.S. manufactured gas turbines to stay competitive, their NO_x levels must be below 10 ppm and their thermal efficiencies should approach 60%. Current technology is being stretched to achieve these goals.

The twin goals of high efficiency and low NO_x emissions require extending the operating range of current gas turbines. Higher efficiency requires operation at higher pressures and temperatures. Lower NO_x emissions requires lower flame temperatures. Lower flame temperatures can be achieved through partially to fully premixed combustion. However, increased performance and lower emissions result in a set of competing goals.

In order to achieve a successful compromise between high efficiency and low NO_x emissions, advanced design tools must be developed. One key design tool is a computationally efficient, high pressure, turbulent flow, combustion model capable of predicting pollutant formation in an actual gas turbine. Its development is the goal of this program.

Achieving this goal requires completion of three tasks. The first task is to develop a reduced chemical kinetics model describing NO_x formation in natural gas-air systems. The second task is to develop a computationally efficient model that describes turbulence-chemistry interactions. The third task is to incorporate the reduced chemical kinetics and turbulence-chemistry interaction models into a commercially available flow solver and compare its predictions with experimental data obtained under carefully controlled conditions so that the accuracy of model predictions can be evaluated. The resulting design tool will be used by U.S. gas turbine manufacturers to design the next generation of lean premixed engines. Such lean premixed flame combustors will satisfy the low NO_x emission needs of the Advanced Turbine Systems (ATS) being developed by several industries under the sponsorship of the Fossil Energy (FE) program of the U.S. Department of Energy (DOE).

Objectives

The overall objectives of the research at Purdue are to:

Research sponsored by the U.S. Department of Energy's Morgantown Energy Technology Center, under contract DE-FC21-92MC29601 with South Carolina Energy Research and Development Center, 386-2 College Avenue, Clemson, SC 29634-5180, Dr. Daniel B. Fant, Telefax: 803-656-2267. Purdue University subcontract No. 93-01-SR009.

- obtain a reduced mechanism description of high pressure NO formation chemistry using experiments and calculations for laminar lean premixed methane air flames,

- develop a statistical model of turbulence - NO chemistry interactions using a Bunsen type jet flame, and

- utilize the high pressure chemistry and turbulence models in a commercial design code, then evaluate its predictions using data from an analog gas turbine combustor.

Work to date has resulted in the following achievements:

- spatially resolved measurements of NO in high-pressure high-temperature flat flames, plus evaluation of the influence of flame radiation on the measured temperature profile

- measurements of temperature and velocity PDFs for a turbulent methane/air flame were obtained for the first time, under operating conditions which allow their study in the distributed regimes, and the increase in $EINO_x$ with equivalence ratio predicted using a chemical kinetics model

- simulation of non-reacting combustor flow fields from ambient to elevated pressure and temperature conditions and comparison of those results with experimental velocity profiles.

Approach

Work is divided into three tasks: reduced chemical kinetics model, turbulence-chemistry interaction model, analog gas turbine modeling and experiments.

Reduced Kinetics Model

In order to determine optimal combustion parameters to minimize pollutants and maintain high efficiency in gas turbine engines, it is necessary to understand the chemical kinetics involved in the production of NO in high-pressure, natural-gas fired, premixed systems. In addition, accurate *in-situ* measurements of NO in these flames are required to verify any computer modeling scheme.

This paper describes recent work in improving both the accuracy of NO measurements in lean-high pressure $CH_4/O_2/N_2$ flames and the accuracy of kinetic modeling for these same conditions. Specifically, this portion of the research is involved in the validation and development of simplified kinetic models for predicting NO formation in these high-pressure lean conditions. To meet these objectives we are measuring NO concentrations in the post-flame zone of a flat, laminar, premixed $CH_4/O_2/N_2$ flame using laser-induced fluorescence. We are modeling NO production using the Sandia laminar premixed flame code. The flame code is being used not only to predict overall NO production in these flames, but to also help determine which NO production pathways are most important in the high-pressure, lean conditions relevant to this study. Knowledge of the pressure dependence of each pathway will be helpful in the later development of a reduced mechanism which may be included in turbulence models for determining NO formation in more realistic turbulent combustors.

In the last six months steps have been taken to improve the accuracy of both the LIF measurements and the modeling, as will be discussed later in this paper.

The laser system and optical layout used in performing the LIF measurements of NO are described elsewhere [Reisel *et al.*, 1993]; thus, only a brief summary will be presented here.

Excitation of NO is achieved through use of the $Q_2(26.5)$ transition of the NO molecule.

A pulsed ultraviolet laser beam is directed over a burner located inside the high-pressure combustion facility described by Carter *et al.* [Carter *et al.*, 1989]. The pressure vessel has four optical ports, two of which provide the optical access and exit for the laser beam through the combustion facility.

For fluorescence detection, we make use of an optical port perpendicular to the laser entrance and exit ports. The fluorescence is focused on the entrance slit of a 1/2-m monochromator. The broadband fluorescence signal encompasses a spectral width of 3 nm and is detected over a spectral region centered at 236 nm. This location and spectral width corresponds to the $\gamma(0,1)$ band of NO.

When performing a linear LIF measurement, one must consider the effects of both laser power fluctuations and quenching variations on the fluorescence signal. Corrections for laser power fluctuations can be made by normalizing the fluorescence signal using the measured laser power. Quenching variations could be handled in a similar manner; however, measurement of the quenching rate coefficient is not a trivial task. Comparisons of measurements obtained using both LIF and laser-saturated fluorescence (LSF) in atmospheric $CH_4/O_2/N_2$ flames demonstrate that the quenching variation is not significant. Additionally, the quenching rate coefficient has been modeled for each of the pressures used in this study. Results for each pressure predict less than a 15% change, with respect to the calibration flame, across our range of equivalence ratios.

Modeling of the chemical kinetics in these flames was performed using the Sandia, steady, laminar, one-dimensional, premixed flame code [Kee *et al.*, 1985]. The mechanism used as the chemical kinetics input into the computer model is based on the comprehensive mechanism assembled by Glarborg *et al.* [1986] as modified by Drake and Blint [1991]. This reaction mechanism considers 49 species and over 200 elementary reactions.

A burner surface temperature of 300 K is used as a boundary condition to simulate the heat loss to the water-cooled burner. A temperature profile generated via solution of the energy equation was used initially for modeling NO production trends. Well-resolved, experimentally measured temperature profiles are not easily obtained at high pressures owing to the close proximity of the flame front to the burner surface. While the calculated temperature profiles will not agree precisely with the actual temperature profiles (leading to some potential errors in quantitative agreement), the calculated post-flame temperatures appear to agree sufficiently with the measured post-flame temperatures so as to allow for an accurate assessment of the pressure trends. Steps taken to obtain more quantitative results are described later in this paper.

Turbulence-Chemistry Interaction Model

Practical gas turbine combustors involve turbulent flames and the residence times available are much smaller than those in the laminar flames studies by the above authors. Analytical studies on premixed turbulent flames have not provided complete insight into their structure. The analytical studies were based on assumptions that are hard to justify. A better study of the turbulent premixed flames can be done by using experimental data in the form of probability density functions (PDFs), length scales etc. of the dependent variables as input into the chemical kinetics models, thereby reducing the complexity of the modeling effort.

The conventional approaches to describing reacting flows in combustors such as gas turbine engines involve moment closure methods [Jones

and Whitelaw, 1982], Monte-Carlo or stochastic methods [Ghoniem *et al.*, 1982, Kerstein, 1988], and PDF methods [Kollman, 1990; Pope, 1991].

The moment closure methods involve developing a hierarchy of equations for the different moments for the variables of interest (velocity, concentrations, temperature, etc.). Normally only the first two moments are considered since beyond this the number of modeling constants increases drastically without providing a correspondingly more accurate solution to the governing equations. However, for non-linear processes such as chemical kinetics, describing the temperature by two or even four moments leads to inaccuracies in the solutions for the chemical processes.

Monte-Carlo or stochastic methods include the Random Vortex methods of Ghoniem *et al.* [1982] and the Linear Eddy Model of Kerstein [1988]. These methods have been used with limited success to predict the scalar mixing of fluids. However, in application to reacting flows, they have problems with convergence, produce large errors due to the limited number of realizations and require extensive modeling efforts which are problem specific [Givi, 1987]. In addition, stochastic methods do not guarantee the conservation of mass, momentum and energy and require ad-hoc modeling for diffusion.

Conventional PDF methods [Kollman, 1990; Pope, 1991] are based on deriving transport equations for the PDFs of the variables of interest. The derivation results in an increase in dimension of the governing equations and the solution procedure requires Monte-Carlo simulations with the inherent problems discussed above. In addition, the turbulent convection and molecular diffusion terms have to be modeled, restricting their use to simple problems [Givi, 1987].

Recently, we developed a new approach called the Discrete Probability Function (DPF) method to solve statistical transport equations in the context of radiative heat transfer [Sivathanu and Gore, 1993]. The DPF method relies on the representation of the PDF transport equation using discrete parcels that are affected by convection and diffusion. The transport equations are solved for notional parcels representing realizable values of boundary conditions and source functions, while the probabilities of the solution so obtained are calculated from statistical laws. The DPF method, along with a model of the molecular diffusion process using spatial series analysis was subsequently used to successfully capture the scalar mixing in a shear layer [Sivathanu and Gore, 1994] and evaluated using data from Yoon and Warhaft [1990] and Bilger *et al.* [1991].

To apply the DPF method for calculating the pollutant production in a turbulent premixed flames, the statistics of temperature are required to take into account the non-linear dependence of the Arrhenius reaction rates on temperature. There have been relatively few measurements of the fluctuating temperature in premixed turbulent flames despite the importance of such information for modeling pollutant emission.

Yoshida [1981] studied the structure of hydrogen pilot stabilized premixed flames with equivalence ratios of 0.8 using compensated thin wire thermocouples. From their measurements, they found that the fluctuating temperature increases and reaches a maximum in the middle of the flame zone and decreases to zero outside the flame zone. The temperature fluctuations in the flame zone were found to be close to the predictions of a wrinkled laminar flame model, implying a bimodal PDF for temperature. Yanagi and Mimura [1981], who also studied pilot stabilized natural gas flames using thermocouples, came to the same conclusion.

However, Pita and Nina [1986] concluded that catalytic effects impose severe limitations on the accuracy of mean and fluctuating

temperatures measured with coated or uncoated thermocouples. Accurate measurements of temperature are need to model the NO_x formation kinetics in turbulent premixed flames. Therefore, a thin filament pyrometer [Vilimpoc and Goss, 1988] was used to measure the fluctuating temperatures in the present work.

Based on the above observations, the objectives of the present work were to measure the fluctuating temperatures in turbulent premixed flames and to use the PDF of the temperature obtained from the measurement to predict the emission index of NO_x.

Temporally and spatially resolved measurements of velocity and temperature were obtained in a co-flow burner, whose sketch is shown in Fig. 1. Premixed fuel and air was sent through a 15 mm diameter inner tube, which is surrounded by a 100 mm diameter annulus for the co-flow air. Wire mesh and glass beads were used to straighten the flow. The premixed flame was stabilized by passing an annular co-flow of hydrogen through a pilot flame burner. The fuel-tube was cooled by passing water through a cooling coil surrounding the inner tube. The length of the fuel tube was 600 mm to ensure a completely developed pipe flow at the exit of the burner.

The mass flow rates of the fuel, the hydrogen used for the pilot flame and the co-flowing air were measured using calibrated rotameters. The mass flow rate of the air used to premix with the fuel was measured using a calibrated choked orifice. Two different heat release rates (4.2 kW and 8.4 kW) and two equivalence ratios (0.8 and 1.0) for each heat release rate were selected to obtain a total of four premixed turbulent flames. The co-flow of air for all flames was fixed at 0.5 g/s and the mass flow rate of the hydrogen used for the pilot flame was 2 mg/s. The Reynolds number based on cold gas properties at the fuel tube burner exit varied between 7000 and 17000.

The instantaneous temperatures were measured using a 15 mm SiC filament stretched inside the flame [Vilimpoc and Goss (1988]. A schematic of the experimental setup for the thin filament pyrometry technique is shown in Fig. 2. The radiation emitted by the SiC filament was imaged onto a cooled InSb detector (spectral window from 1200 to 5700 nm) through a chopper, aperture, and imaging lenses. The signal was amplified, phase locked, digitized and stored in a laboratory computer at 5000 Hz. The system was calibrated using the known temperatures from a laminar flame. The small size of the filament, low thermal conductivity and high emissivity offered good spatial and temporal response. The resulting data were used to obtain the PDFs of temperatures at all locations within the flames.

The radial and axial velocities were measured using a single component, dual beam Laser Doppler Velocimeter (LDV). Three pollutant species, NO_x, CO and UHC were measured by sampling the exhaust stream using Thermo Environmental Inc. chemiluminescent, gas correlation, and flame ionization analyzers respectively. CO_2 mole fraction was measured using a Rosemount Analytical NDIR CO_2 analyzer. The mole fractions of the pollutant species measured by the analyzers were converted to mass fractions. The mass fractions and CO_2 concentrations were used to find the emission index of the pollutant species.

The two dimensional conservation equation for the mass fraction of NO (Y_{NO}) in a turbulent reacting flow is:

$$\frac{\partial \rho Y_{NO}}{\partial t} + \frac{\partial \rho u Y_{NO}}{\partial x} + \frac{1}{r}\frac{\partial \rho r v Y_{NO}}{\partial y}$$

$$= \frac{\partial}{\partial x}\left(\rho D \frac{\partial Y_{NO}}{\partial x}\right) + \frac{1}{r}\frac{\partial}{\partial r}\left(\rho r D \frac{\partial Y_{NO}}{\partial r}\right) + \dot{\omega}''' \quad (1)$$

where, ρ is the density, u is the velocity in the axial (x) direction, v is the velocity in the radial (r) direction, D is the molecular diffusivity and $\dot{\omega}'''$ is the production rate of NO in kg/m^3-s.

Numerical simulations for calculating the PDF of Y_{NO} at all locations within the flame is computationally intensive. However, the emission index of NO_x can be calculated if the axial mass flux of NO is known at all locations. The total mass flux of NO $\left(\dot{m}_{NO}, \text{ in kg/s}\right)$ at any axial location can be calculated as:

$$\dot{m}_{NO} = \int_0^R 2\pi u r \rho Y_{NO} dr \qquad (2)$$

where R is the boundary of the computational domain beyond which the mass fraction of Y_{NO} is zero.

Neglecting axial diffusion the change in mass flux of NO for an axial spacing of Δx can be obtained from Eq. (1) and (2) as:

$$\Delta\dot{m}_{NO} = \Delta x \int_0^R 2\pi r \dot{\omega}''' dr \qquad (3)$$

The changes in the NO mass flux from the exit to the last axial location (where the production rate term goes to zero) are added together to give the overall mass flux of NO from the flame. This information along with the fuel flow rate is used to obtain the $EINO_x$ (NO_x emission index) for the flame.

The reaction rate term in Eq. (3) is obtained from Rokke *et al.* [1992], and includes the Zeldovich, prompt and nitrous oxide mechanisms. The concentrations of the major species are required to calculate the production of NO [Rokke *et al.*, 1992] and are obtained using state relationships as a function of temperature assuming the reaction rate progress variable for the major species is one.

The temperature at any location is fluctuating as a function of time. Therefore, to obtain the time averaged mass flux of NO, $\langle\Delta\dot{m}_{NO}\rangle$, Eq. (3) is multiplied by the PDF of T and integrated over the entire range of T as follows:

$$\langle\Delta\dot{m}_{NO}\rangle = \Delta x \int_{T_{min}}^{T_{max}} \int_0^R 2\pi r \dot{\omega}'''(T) PDF(T) dr dT \qquad (4)$$

where T_{min} and T_{max} are the minimum and maximum temperatures observed at any radial location r. For the four different flames, Eq. (4) was numerically integrated from x = 0 to x = 200 mm at which location the instantaneous peak temperatures were below 1100 K and NO production was negligible. 80 grids were used in the axial direction and the PDF of T was discretized by 50 bins. Doubling either the number of x-grids or the number of bins resulted in less than 1% change in $EINO_x$.

Analog Gas Turbine Modeling and Experiments

Non-reacting flow velocity measurements were made in an axisymmetric combustor at preheated and pressurized conditions. These measurements were used to evaluate the accuracy of non-reacting numerical simulations performed using FLUENT.

The experimental combustor is axisymmetric to facilitate modeling. A 2.54 cm diameter inlet feeds a 7.62 cm diameter dump zone that is fitted with quartz windows to allow optical access for LDV measurements, as well as access for gas sampling probe measurements to be performed during the next phase of work. A

water cooling jacket surrounds the combustor casing.

Preheated, high pressure, unvitiated air is supplied from storage tanks to a non-contact heat exchanger and on to the combustor. The air flow rate is measured using a choked orifice.

Only non-reacting results are reported here, so no fuel is used. However, in future work fuel (methane) will be supplied by a bank of conventional high pressure gas cylinders. The fuel flow rate will be measured using a choked orifice.

Air and fuel are mixed upstream of the combustor via a radial "sting." The extent of mixing will be assessed using Mie scattering.

A honeycomb flow straightener and 2.25:1 area ratio contraction are located upstream of the combustor dump plane so that the velocity profile is sensibly flat at the dump plane. The flatness of that profile is checked using LDV.

Combustor pressure and inlet velocity are varied by controlling the rates of air and fuel supplied to the combustor and restricting the diameter of the combustor at its exit plane. The restriction consists of a stainless steel cap and one of a number of graphite nozzles which serve to choke the exit flow.

The combustor has been operated at pressures of 1, 2, 5, 10 and 15 atm. Inlet velocity is nominally 10 m/s.

The LDV system is that of Gould [1989]. It was operated in the forward scatter mode as a single component instrument. Frequency shifting was employed to allow unambiguous velocity measurement in regions of recirculation and to eliminate incomplete signal bias.

Seeding was accomplished by distributing Al_2O_3 particles into a secondary air stream via a high-pressure seeder. The seeded secondary stream was introduced to the main air flow upstream of the fuel injection sting. The secondary air mass flow rate was also measured using a choked orifice.

Experimental results are compared to numerical results generated using FLUENT. FLUENT uses the finite volume approach to discretize the equations of motion.

FLUENT has flexibility to allow inclusion of a number of submodels that describe various transport phenomena. These include the ideal gas equation of state, Fourier's Law of heat conduction, Fickian mass diffusion, and the assumption of Newtonian fluids.

There are three options for turbulence modeling: k-ε, renormalization group (RNG) k-ε, and the Reynolds' stress model (RSM). Previous work completed as part of this program indicated only slight differences in the level of agreement when comparing model simulations based on the three turbulence models with LDV data. Consequently, the "standard" k-ε model was chosen because it requires the least computational time to converge to a solution.

Results

Reduced Kinetics Model

Using the LIF apparatus described above, NO concentrations have previously been measured in high-pressure, premixed, laminar CH_4/O_2/N_2 flames. To enhance the accuracy of these measurements, we have improved the precision of our calibration system by installing a new high-pressure mass-flow controller system for delivery of the calibration gas. Of additional concern for the accuracy of these measurements is the effect of fluorescence interferences due to species other than NO. Specifically, O_2 fluorescence can cause a significant background offset which must be accounted for in LIF

measurements of NO, especially at the lean, high-pressure conditions investigated here.

We studied the effect of O_2 interferences in nitrogen-air flames by obtaining fluorescence excitation and detection scans in the post-flame zone of a non-cooled 3.76 dilution ratio, 0.6 equivalence ratio, flat, premixed flame stabilized on a porous ceramic plug. The excitation scans show that the $Q_2(26.5)$ transition is not in the same region as any distinct interference feature, nor is it concurrent with any other NO feature. These traits, combined with this transition's relatively temperature-insensitive Boltzmann fraction make $Q_2(26.5)$ excitation a good choice for fluorescence measurements.

However, even though this excitation transition avoids major interference features, some fluorescence and Raman features will be excited at any wavelength in this region. To further avoid these interferences, it is necessary to choose a detection strategy that collects as much NO related signal as possible while rejecting non-NO interferences.

Thus, detection scans were obtained at 1 and 6 atm in both $CH_4/O_2/N_2$ and $CH_4/O_2/Ar$ flames. The argon diluted flames, shown in Figs. 3a and b, lack the NO signal and thus give a good indication of the location and magnitude of non-nitrogen related interferences. The nitrogen diluted scans of Figs. 3c and d contain the interference features as well as those due to N_2 and NO.

These detection scans are presented on a relative fluorescence basis by normalizing the peak signal to 1000. The $\gamma(0,1)$, $\gamma(0,2)$ and $\gamma(0,3)$ bands of NO are apparent in Figs. 3c and d at approximately 236, 246, and 258 nm, respectively. A strong N_2 Stokes Raman scattering signal is also seen at ~238 nm [Eckbreth, 1988] in the nitrogen-flame detection scans. An H_2O Raman line occurs within the $\gamma(0,2)$ band of NO, ~246 nm. Thus the $\gamma(0,2)$ band of NO would be a poor choice for NO detection. Also evident in these scans are the large interferences due to O_2 fluorescence seen as doublets before the $\gamma(0,1)$ band, between the $\gamma(0,1)$ and $\gamma(0,2)$ bands and in the middle of the $\gamma(0,3)$ band of NO. These interferences would also make the $\gamma(0,3)$ band of NO a poor choice for NO detection.

What these scans show us is that interferences can largely be avoided in LIF measurements of NO in lean methane-air flames, if the $Q_2(26.5)$ transition of NO is used for excitation in conjunction with detection of a 2 to 3 nm portion of the $\gamma(0,1)$ band of the NO molecule. However, at higher pressures and temperatures and in lower dilution ratio flames, the O_2 background can become significant even with the above excitation/detection scheme. To attain more accurate LIF measurements at these extreme conditions, correction procedures are currently being developed to experimentally measure the background and subtract it from the measured fluorescence signal.

In earlier reports, we have described the results of our extensive modeling effort using the Sandia 1-D premixed flame code to predict NO formation in the flames we have investigated experimentally. One issue which prevented accurate predictions of NO formation in high-pressure $CH_4/O_2/N_2$ flames was the inability of the flame code to adequately predict the temperature field above the burner surface, especially at high pressures. One cause for this deficiency was the failure of the model to account for radiative heat losses from the flame to the surroundings, which should become very significant at higher pressures. Our first step to alleviate this problem was the addition of a simple radiative heat loss model to the Sandia 1-D Premixed Flame Code. Assuming that these flames are in the optically-thin regime, a radiation source term was calculated using a Planck mean temperature coefficient. This coefficient was calculated from a narrow band model using

the RADCAL program [Grosshandler, 1988]. Preliminary results for flames at atmospheric pressure are shown in Fig. 4.

Turbulence-Chemistry Interaction Model

The effect of the varying the amount of hydrogen used for the pilot flame on the emission indices of UHC, CO, NO and NO_x is shown in Fig. 5. All the flames used in the present study blow off if the hydrogen pilot is stopped. The amount of hydrogen required increases as the jet velocity increases. This is partly due to the higher velocities and also to the lower temperatures for the leaner flames. If the pilot flame is too small, UHC and CO levels increase very rapidly as the flame becomes unstable, and any further decrease of the hydrogen flow would blow off the flame.

The emission index for NO and NO_x increases with increasing hydrogen flow rate. The increase in adiabatic temperature produced due to combustion of hydrogen in the pilot flame is responsible for the increased levels of NO and NO_x. The higher temperature also promotes complete combustion, leading to lower emission indices for CO and UHC. All four flames used 2 mg/s of H_2 for the pilot flame. This low amount of hydrogen results in only about a 20% increase in $EINO_x$ allowing critical evaluation of the chemical kinetics model.

The PDFs of axial velocity, for five different radial locations and 60 mm above the burner, for the 4.2 kW lean premixed turbulent flame are shown in Fig. 6. The mean velocity decreases from the center line towards the edge of the flame, and the RMS velocity remains almost constant across the flame width. At locations close to the high temperature zone (r = 12 mm and r = 14 mm), the fluctuation in axial velocity is about 30 % of the mean. The PDF at the center is narrow and symmetric around the mean value. The effects of intermittency are evident for the PDF at r = 16 mm since the PDF has a long tail for positive velocities and is not symmetric around the mean value. Outside the flame zone, the mean and the fluctuations in velocity decrease rapidly. The shapes of the velocity PDFs are nearly Gaussian.

The PDFs of temperature at the same five radial locations for the 4.2 kW lean premixed turbulent flame are shown in Fig. 7. The mean temperature at the center is very low, rises to a maximum of 1755 at r = 12 mm and then decreases outside the flame. Interestingly, the fluctuations are minimum at the flame surface, indicating that the flame sheet is relatively stationary at this point despite the high level of axial velocity fluctuation. Close to the flame sheet, the peak temperatures reach close to adiabatic values. However, such high temperature excursions are not seen at the edge of the flow or at the center. In addition, the fluctuations increase towards the edge of the flow due to intermittency. At the center line of the jet and an axial location of 60 mm, the temperature is very low and below 900 K almost all the time.

There are a number of phase diagrams that define various combustion regimes in terms of length and velocity scales [Borghi, 1984; Williams, 1985; Peters, 1986]. In this work, we follow the analysis of Peters [1986] and plot the ratio of the RMS of velocity (u') to the laminar flame speed (S_L) as a function of the ratio of the integral length scale (l_t) to the laminar flame thickness (l_F), as shown in Fig. 8. The turbulent Reynolds (Re), Damkohler (Da) and Karlovitz (Ka) numbers are given by:

$$Re = u' l_t / \upsilon \tag{5}$$

$$Da = t_t / t_F = S_L l_t / u' l_F \tag{6}$$

and

$$Ka = t_F/t_k = l^2_F/l^2_F = \epsilon^{1/2} l_F/\upsilon^{1/2} S_L \quad (7)$$

respectively where n is the kinematic viscosity, t_t is the integral time scale, and ε is the turbulent kinetic energy. Based on the above definitions, we can derive the following relationship for the three non-dimensional numbers, Re, Da and Ka, in terms of u'/S_L and l_t/l_F as [Peters, 1986]:

$$u'/S_L = Re \left(l_t/l_F\right)^{-1} \quad (8)$$

$$u'/S_L = Da^{-1} \left(l_t/l_F\right) \quad (9)$$

$$u'/S_L = Ka^{2/3} \left(l_t/l_F\right)^{1/3} \quad (10)$$

The regimes of laminar flames (Re < 1) and well stirred reactor (Da < 1) are not of interest for the present work. Among the three remaining regimes, the wrinkled and corrugated flames belong to the flame regime which is characterized by the inequalities Re > 1 (turbulence), Da > 1 (fast chemistry) and Ka < 1 (sufficiently weak flame stretch). In the flamelet regime the Kolmogorov length scale is greater than the flame thickness, so the smallest eddies do not penetrate the flame sheet and we get thin laminar flamelets. u' is interpreted as the circumferential velocity of the largest eddies and when $u' < S_L$, these eddies can not convolute the flame front to form the multiply connected flame sheets. When $u' > S_L$, multiple flame sheets are formed giving rise to corrugated flamelets.

The boundary of the distributed reaction zone is given by Ka = 1 and can be expressed as the condition where the flame thickness is equal to the Kolmogorov scale. The distributed reaction zone is bounded by Re > 1; Da > 1 and Ka > 1. In the distributed reaction zone, Ka > 1, the Kolmogorov scale is smaller than the flame thickness and the smallest eddies can enter the flame structure thereby broadening the flame structure.

All previous measurements in the literature fall within either the wrinkled flamelet or corrugated flamelet regimes. The present work is the first time that flames stabilized (due to hydrogen pilot flame) in the distributed reaction regime are accessible.

The predictions and measurements of $EINO_x$ normalized by its value at equivalence ratio of 1 is shown in Fig. 9. The chemical kinetics model captures the change in $EINO_x$ with equivalence ratio quite well. However, the absolute values are about 330% higher for the 4.2 kW flame and 40% higher for the 8.4 kW flame. Two sets of predictions are also shown in Fig. 9. The open triangle represents predictions of $EINO_x$ obtained using the measured temperature PDF. The open circles represents predictions obtained using a Gaussian PDF, with the maximum temperature being limited to the adiabatic flame temperature. The data is represented by the solid circles. Both sets of predictions capture the increase in $EINO_x$ with equivalence ratio quite well. The predictions are shown only for two equivalence ratios since measurements of the temperature PDFs are available for only four flames.

Analog Gas Turbine Modeling and Experiments

Experimental data at pressures from 1 to 15 atm and temperatures from 295 to 480 K was obtained using our high pressure analog gas turbine combustor operating under non-reacting conditions. Table 1 illustrates the pressure-temperature combinations that have been investigated. Velocity data obtained at these conditions was used to evaluate the pressure and temperature scaling capabilities of FLUENT. Particular attention was paid to the influence of operating pressure and temperature on the flow field, and the agreement between experimental data and numerical simulations as these two parameters were varied.

Experimental data and model predictions for the cases listed in Table 1 are presented in Fig. 10 through 13. Experimental data were checked for symmetry by scanning the LDV probe volume across the combustor diameter. Velocity profiles from the two radii were then compared at a number of axial locations and the root-mean-square (rms) deviation, defined as

$$\frac{1}{N}\sqrt{\sum_{i=1}^{N}\frac{\left(u_{ir}-u_{il}\right)^2}{\left[\left(u_{ir}+u_{il}\right)/2\right]^2}}, \qquad (11)$$

computed. Here u_{ir} is the axial velocity at radial position i for the right hand radius, u_{il} is the axial velocity at radial position i for the left hand radius, and N is the number of radial positions at which data were acquired. The root mean square deviation between sides was less than 22%. The experimental data were also checked for repeatability by acquiring velocity fields on different days. The rms deviation between velocity fields acquired on different days, defined analogously to Eqn. (11), was 21%.

Table 1. Pressure-Temperature Conditions at Which LDV Data Were Obtained

Pressure, atm	Temp., K	Reynolds number, x10^{-4}	Dump velocity, m/s
1	295	1.8	9.8
2	295, 383	3.6, 2.1	11, 9.8
5	295, 439	9.0, 3.9	11, 9.8
10	295, 450	18, 7.5	11, 9.8
15	294, 477	27, 10	11, 10

Figure 10 illustrates agreement between model predictions and experimental data for a combustor pressure of 2 atm and an inlet temperature of 383 K. The results demonstrate that FLUENT accurately predicts the recirculation zone, present at x/H=2.1 and 4.7, and the decay of the central jet, between x/H=0.1 and x/H=8.3. Discrepancies between model predictions and experimental data exist at x/H=8.3, where FLUENT indicates the recirculation zone has ended and the experimental data shows it to persist, and at x/H=8.3 and 11.8, where FLUENT first under- and then over predicts the persistence of the central jet.

Figure 11 illustrates agreement between model predictions and experimental data for a combustor pressure of 5 atm and an inlet temperature of 439 K. The results demonstrate that FLUENT again predicts the recirculation zone, present at x/H=2.1 and 4.7, and the decay of the central jet. FLUENT simulations are most accurate at non-dimensional axial locations of 11.8 and 14.1. Discrepancies between model predictions and experimental data do exist, however, and are more prevalent than for the 2 atm case. In particular, at x/H=8.3 FLUENT indicates that the recirculation zone persists and the experimental data show it to have ended. Furthermore, at x/H=4.7 and 8.3 FLUENT consistently over predicts the persistence of the central jet.

Agreement between model predictions and experimental data improves as combustor pressure increases to 10 atm, as shown in Figure 12. Figure 12 results demonstrate that FLUENT accurately predicts the location of the recirculation zone and the breakdown of the core flow. A comparison of rms errors between the 5 and 10 atm cases (24 and 21%, respectively) clearly demonstrates the improved accuracy of the 10 atm simulations.

Agreement between model predictions and experimental data is as good for the 15 atm case as it is for the 10 atm case. Figure 13 presents the 15 atm results. Once again, FLUENT is able to accurately predict the location of the

recirculation zone and the breakdown of the core flow. In addition, only minor discrepancies are present, as indicated by an rms error value of less than 21%.

In summary, Fig. 10 through 13 demonstrate that FLUENT is capable of predicting non-reacting, elevated pressure, preheated flow fields for our axisymmetric geometry. Comparison of the results in Fig. 10 through 13 demonstrates that pressure scaling effects on the flowfield are well described. Furthermore, the accuracy of the predictions are seen to improve with an increase in pressure.

Comparison of the results contained in Fig. 10 through 13 with results obtained at corresponding pressures and ambient temperature indicate that temperature scaling effects are also well described. The accuracy of the predictions are observed to improve with increasing inlet temperature.

Applications

Lean premixed flame combustors satisfy the low NO_x emission need of the Advanced Turbine Systems (ATS) being developed by several industries under the sponsorship of the Fossil Energy (FE) program of the U.S. Department of Energy (DOE). Computational tools for the design of lean premixed combustors are presently limited by the lack of understanding of the high pressure NO formation chemistry and turbulence chemistry interactions. The results of this study will improve the competitiveness of U.S. manufactured gas turbines by helping to provide a rational understanding of how engine design influences NO_x production.

Future Work

Our future work will be focused in three areas.

- We will continue to map NO concentrations in our preheated, high pressure flames and accelerate work on the development of a reduced NO kinetic mechanism for use with natural gas fired systems. The reduced kinetic mechanism will be supplied to the Analog Gas Turbine Group.

- We will simulate the energy equation to evaluate the DPF-based turbulence-chemistry interaction model further, make measurements of average major gas species concentration, and incorporate the DPF NO calculations into an industrial code for combustor design. Preliminary measurements of NO concentration statistics are being initiated in collaboration with the Reduced Kinetics Group.

- We will make major species measurements under elevated pressures conditions and simulate the profiles using FLUENT, while incorporating the reduced kinetic mechanism and turbulence - NO chemistry models being developed by the Reduced Kinetics and Turbulence-Chemistry Interaction Groups.

Acknowledgments

The authors gratefully acknowledge the efforts of Dr. Norman Holcombe, METC Project Manager, and Dr. Daniel Fant, Director, AGTSR. This work is supported by DOE contract DE-FC21-92MC29601, through the Morgantown Energy Technology Center. The South Carolina Energy Research and Development Center is the primary contractor, with Purdue University being a subcontractor. The period of performance is 1 September 1993 through 31 August 1996.

The authors also gratefully acknowledge the support of Purdue University's School of Mechanical Engineering, as well as helpful conversations with representatives from Allison

Engine Company, General Electric, Solar Turbines, Inc., United Technologies Research Center, and Westinghouse.

References

Bilger, R.W, Saetran, L.R. and Krishnamoorthy, L.V., 1991, Reaction in a Scalar Mixing Layer," J Fluid Mech., Vol. 233, p. 211.

Borghi R., 1985, "On the Structure and Morphology of Premixed Flames," Recent Advances in Aerospace Sciences, Ed. C. Casci, Plenum, p. 117.

Bowman C.T., 1992, "Control of Combustion-Generated Nitrogen Oxide Emissions: Technology Driven by Regulation," Twenty-Fourth Symposium (Int'l) on Combustion, The Combustion Institute Pittsburgh, PA, p. 859.

Carter, C.D., G.B. King, and N.M. Laurendeau, "A combustion facility for high-pressure flame studies by spectroscopic methods", *Rev. Sci. Instrum.* **60**, 2606 (1989).

Chew T.C., Bray K.N.C., Britter R.E., 1990, "Spatially Resolved Flamelet Statistics for Reaction Rate Modeling," Combust. Flame, Vol. 80, p. 65

Correa S.M., 1992, "A Review of NO_x Under Gas Turbine Conditions," Combust. Sci. Tech., Vol. 87, p. 329.

Drake M.C. and Blint R.J., 1991, "Calculations of NO_x Formation Pathways in Propagating Laminar, High Pressure Premixed CH_4/Air Flames," Combust Sci. Tech., Vol. 75, p. 261.

Eckbreth, A.C., *Laser Diagnostics for Combustion Temperature and Species,* Abacus Press, Cambridge, MA. (1988).

Ghoniem A.F., Chorin A.J., and Oppenheim A.K., 1982, "Numerical Modeling of Turbulent Flow in a Combustion Tunnel," Phil. Trans. R. Soc. Lond., Vol. A 304, p. 303.

Givi, P., 1989, "Model Free Simulations of Turbulent Reacting Flows," Prog. Energy Combust Sci, Vol. 15, p. 1.

Glarborg, P., J.A. Miller, and R.J. Kee, "Kinetic Modeling and Sensitivity Analysis of Nitrogen Oxide Formation in Well-Stirred Reactors", *Combust. Flame* **65**, 177 (1986).

Gould, R.D., "Turbulence Characteristics of an Axisymmetric Reacting Flow," Ph.D. Thesis, Purdue (1987).

Grosshandler, W.L., "Radiative Heat Transfer in Nonhomogeneous Gases: A Simplified Approach", *Int. J. Heat Mass Trans.* **23**, 1447 (1988).

Jones W.P. and Whitelaw J.H., 1982, "Calculation Methods for Reacting Turbulent Flows: A Review," Combust. Flame, Vol. 48, p. 1.

Kee, R.J., J.F. Grcar, M.D. Smooke, and J.D. Miller, A FORTRAN program for modeling steady laminar one-dimensional premixed flames. *Sandia Report SAND* 85-8240 (1985).

Kerstein A.R., 1988, "A Linear-Eddy Model of Scalar Transport and Mixing," Combust. Sci. Tech., Vol. 60, p. 391.

Kollman K.V., 1990, "The PDF approach to Turbulent Flow," Theoret. Comput. Fluid Dyn., Vol. 1, p. 249.

Michaud M.G., Westmoreland P.R. and Feitelberg A.S., 1992, "Chemical Mechanisms of NO_x Formation for Gas Turbine Conditions," Twenty-Fourth Symposium (International) on Combustion, The Combustion Institute Pittsburgh, PA, p. 879.

Moss J.B., 1980, "Simultaneous Measurements of Concentration and Velocity in an Open Premixed Turbulent Flame," Combust. Sci. Tech., Vol. 22, p. 119.

Peters N., 1986, "Laminar Flamelet Concepts in Turbulent Combustion," Twenty-First Symposium (Int'l) on Combustion, The Combustion Institute Pittsburgh, PA, p. 1231.

Pita G.P.A. and Nina M.N.R., 1989, "Errors Induced by Catalytic Effects in Premixed Flame Temperature Measurements," Int'l Conference on Instrumentation in Aerospace Simulation Facilities, IEEE, Piscataway, NJ, p. 179.

Pope S.B., 1991, "PDF method for turbulent reacting flows," Prog. Energy Combust. Sci., Vol. 11, p. 119.

Reisel, J.R., C.D. Carter, N.M. Laurendeau and M.C. Drake, "Laser-Saturated Fluorescence Measurements of Nitric Oxide in Laminar, Flat, $C_2H_6/O_2/N_2$ Flames at Atmospheric Pressure", *Combust. Sci. and Tech.* **91**, 271 (1993).

Rokke N.A., Hustad J.E., and Sonju O.K., 1992, "Scaling of Nitric Oxide Emissions from Buoyancy Dominated Hydrocarbon Turbulent-Jet Diffusion Flames," Twenty-Fourth Symposium (Int'l) on Combustion, The Combustion Institute Pittsburgh, PA, p. 385.

Sivathanu Y.R. and Gore, J.P., 1993, "A Discrete Probability Function Method for the Equation of Radiative Transfer," J. Quant. Spec. Radiat. Transfer, Vol. 49, pp. 269.

Sivathanu Y.R. and Gore J.P., 1994, "Discrete Probability Function Method for a Turbulence Mixing Layer," Fire, Combustion and Hazardous Waste Processing, ASME HTD- Vol. 296, p. 99.

Smallwod G.J., Gulder O.L., Shelling D.R., Deschamps B.M., and Gokalp I., 1995, "Characterization of Flame Front Surfaces in Turbulent Premixed Methane/Air Combustion," Combust. Flame, Vol. 101, p. 461.

Tanaka H. and Yanagi T., 1983, "Cross-Correlation of Velocity and Temperature in a Premixed Turbulent Flame," Combust. Flame, Vol. 51, p. 183.

Vilimpoc V. and Goss L.P., 1988, "SiC-Based Thin-Filament Pyrometry: Theory and Thermal Properties," Twenty-Second Symposium (Int'l) on Combustion, The Combustion Institute Pittsburgh, PA, p. 1907.

Williams F.A., 1985, Combustion Theory, Benjamin Cummins, Menlo Park, CA.

Wu W.S., Kwon S., Driscoll J.F., and Faeth G.M., 1991, "Preferential Diffusion Effects on the Surface Structure of Turbulent Premixed Hydrogen/Air Flames," Combust Sci. Tech., Vol. 78, p. 69

Yanagi T. and Mimura Y., 1981, "Velocity-Temperature Correlation in Premixed Flame," Eighteenth Symposium (Int'l) on Combustion, The Combustion Institute Pittsburgh, PA, p. 1031.

Yoon, K. and Warhaft, Z., 1990, "The Evolution of Grid-generated Turbulence under conditions of Stable Thermal Stratification," J. Fluid Mech., Vol. 215, p. 601.

Yoshida A., 1981, "An Experimental Study of Wrinkled Laminar Flame," Eighteenth Symposium (Int'l) on Combustion, The Combustion Institute Pittsburgh, PA, p. 931.

Yoshida A. and Tsuji H., 1979, Measurements of Fluctuating Temperature and Velocity in a Turbulent Premixed Flame," Seventeenth Symposium (International) on Combustion, The Combustion Institute Pittsburgh, PA, p. 931.

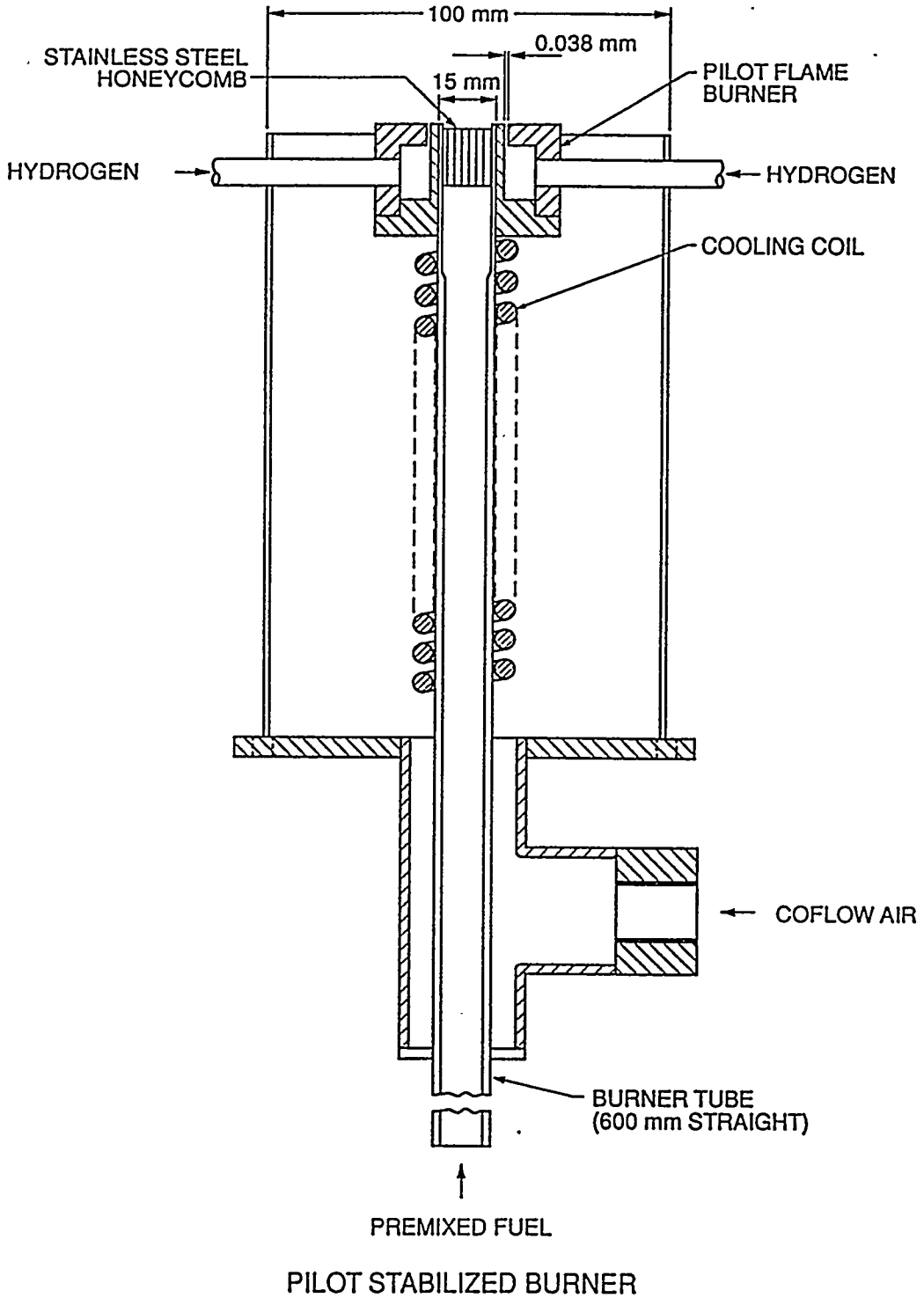

Figure 1. A Schematic of the Turbulent Premixed Burner

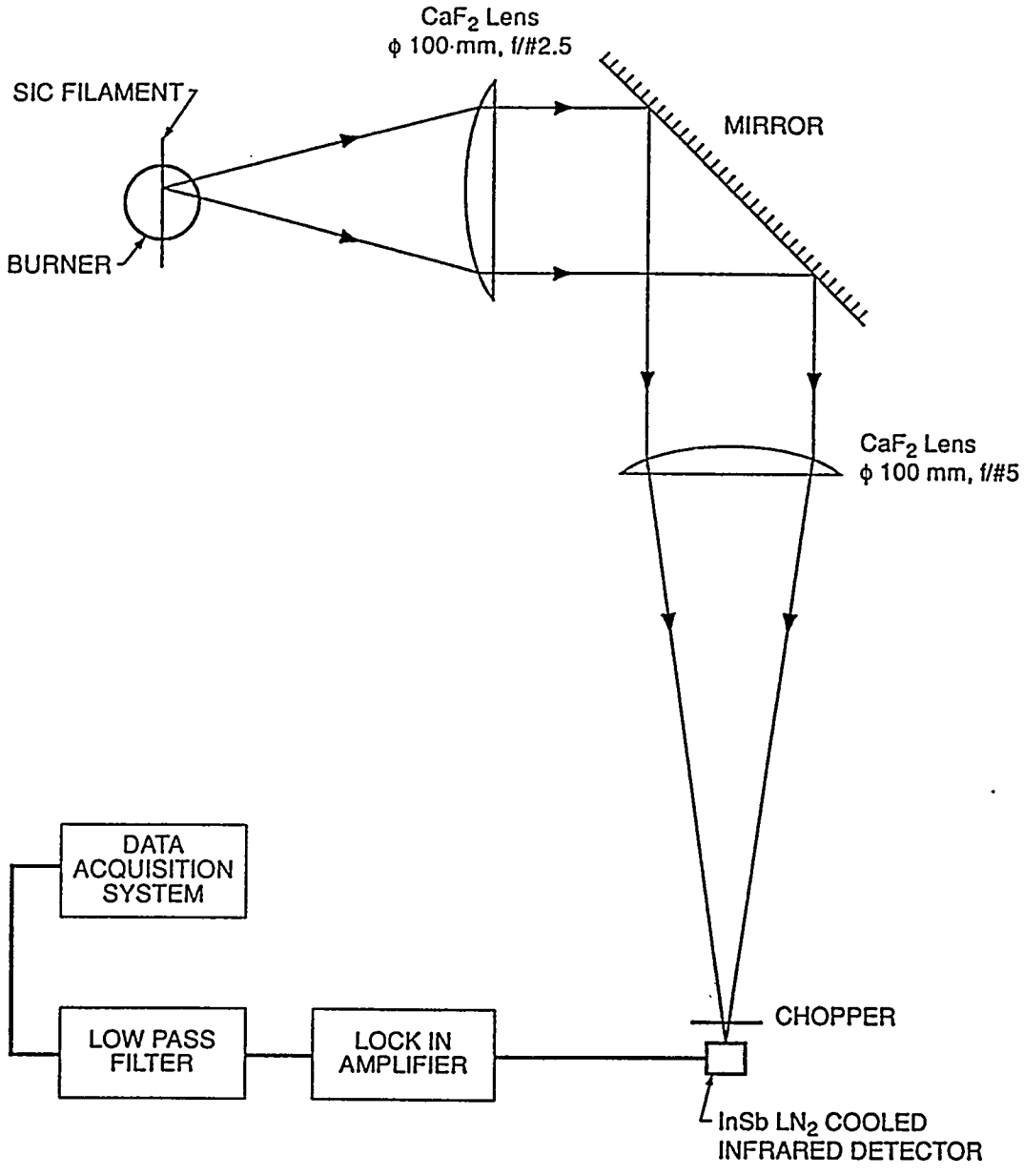

Figure 2. A Schematic of the Thin Filament Pyrometry System

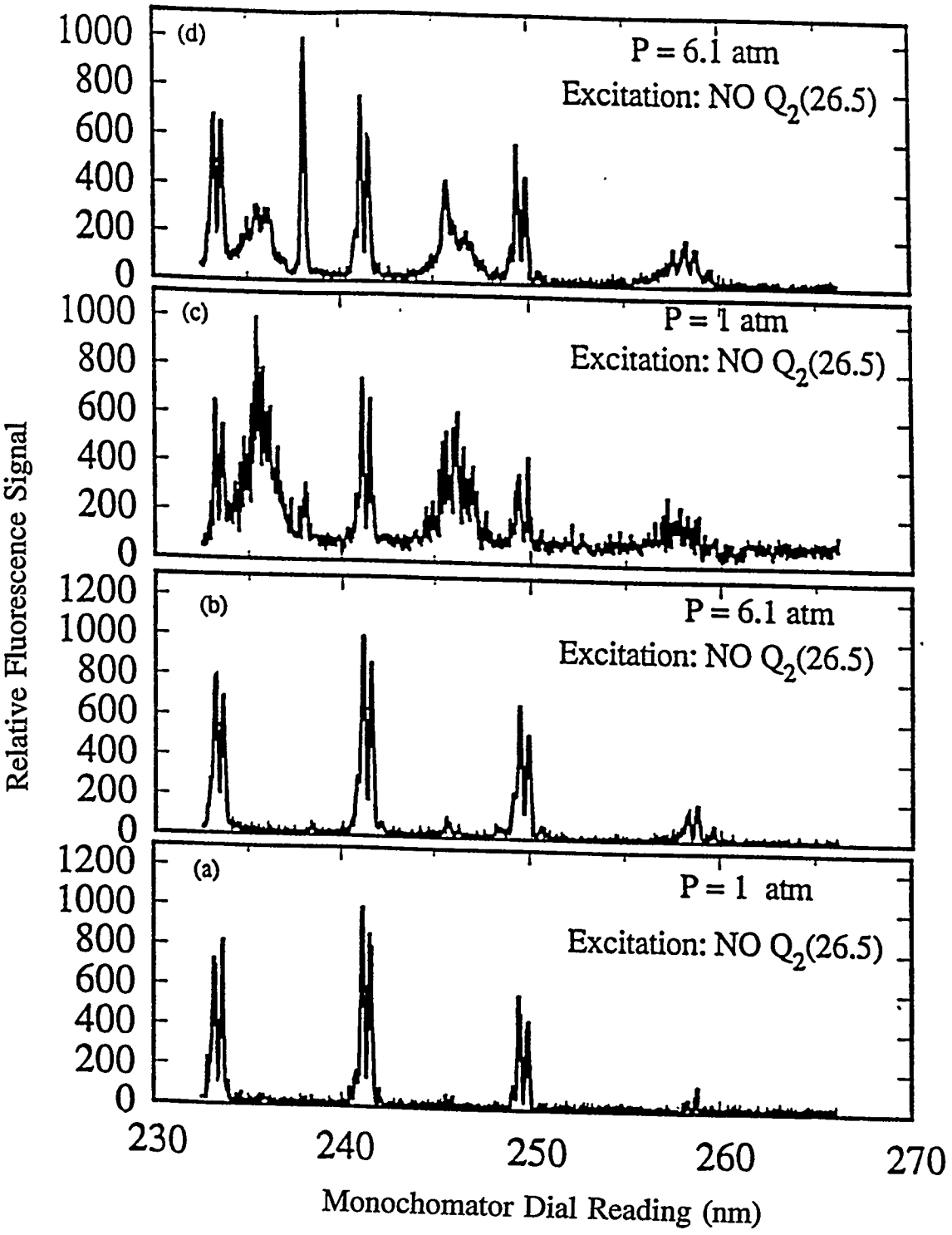

Figure 3. Relative Fluorescence Versus Wavelength for Two Flames at Elevated and Ambient Pressures: a) and b) Are Argon Diluted; c) and d) Contain Nitrogen

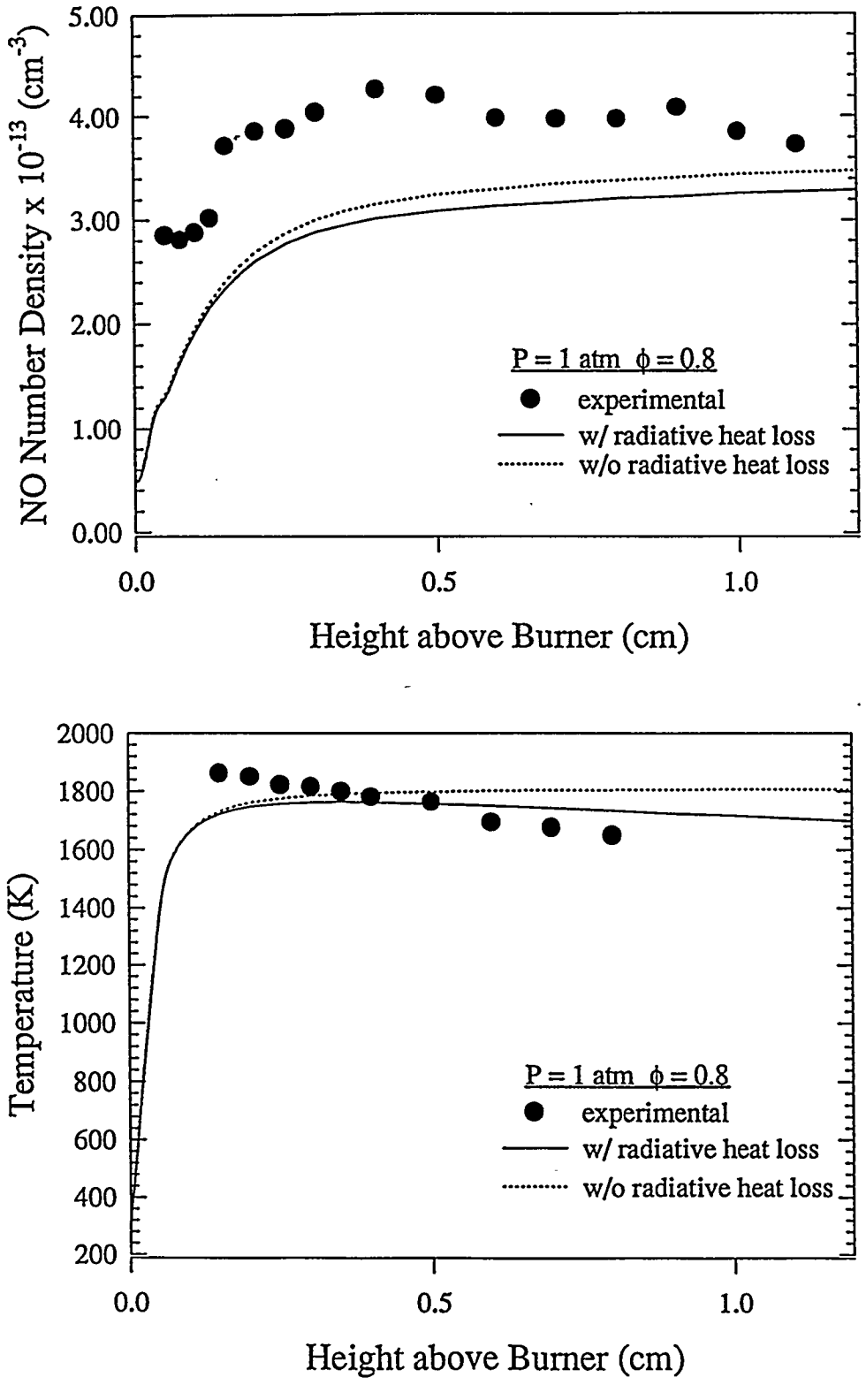

Figure 4. NO Number Density and Temperature Versus Axial Location Above the Burner Surface

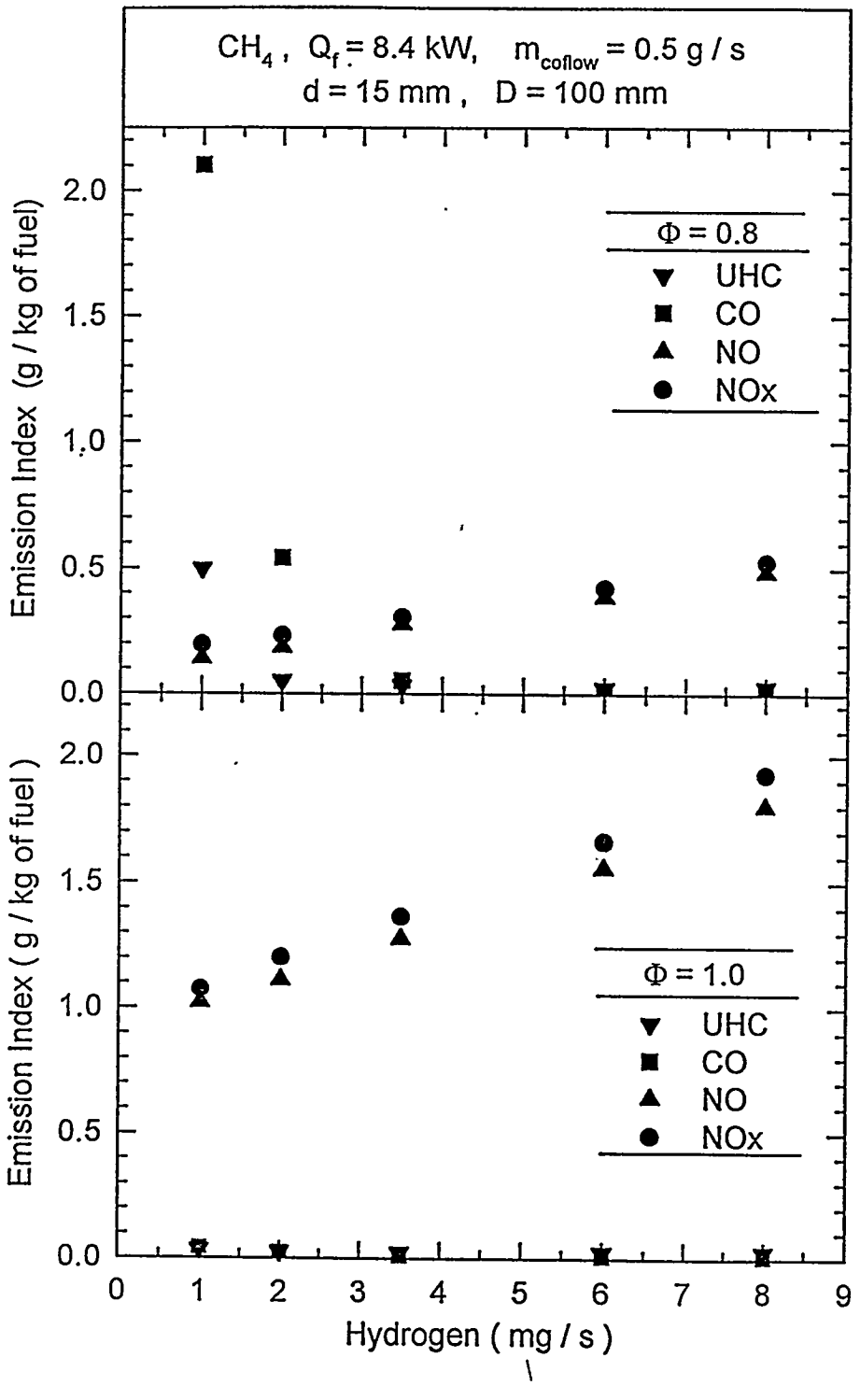

Figure 5. The Effect of Hydrogen Pilot Flame on the Emission Index

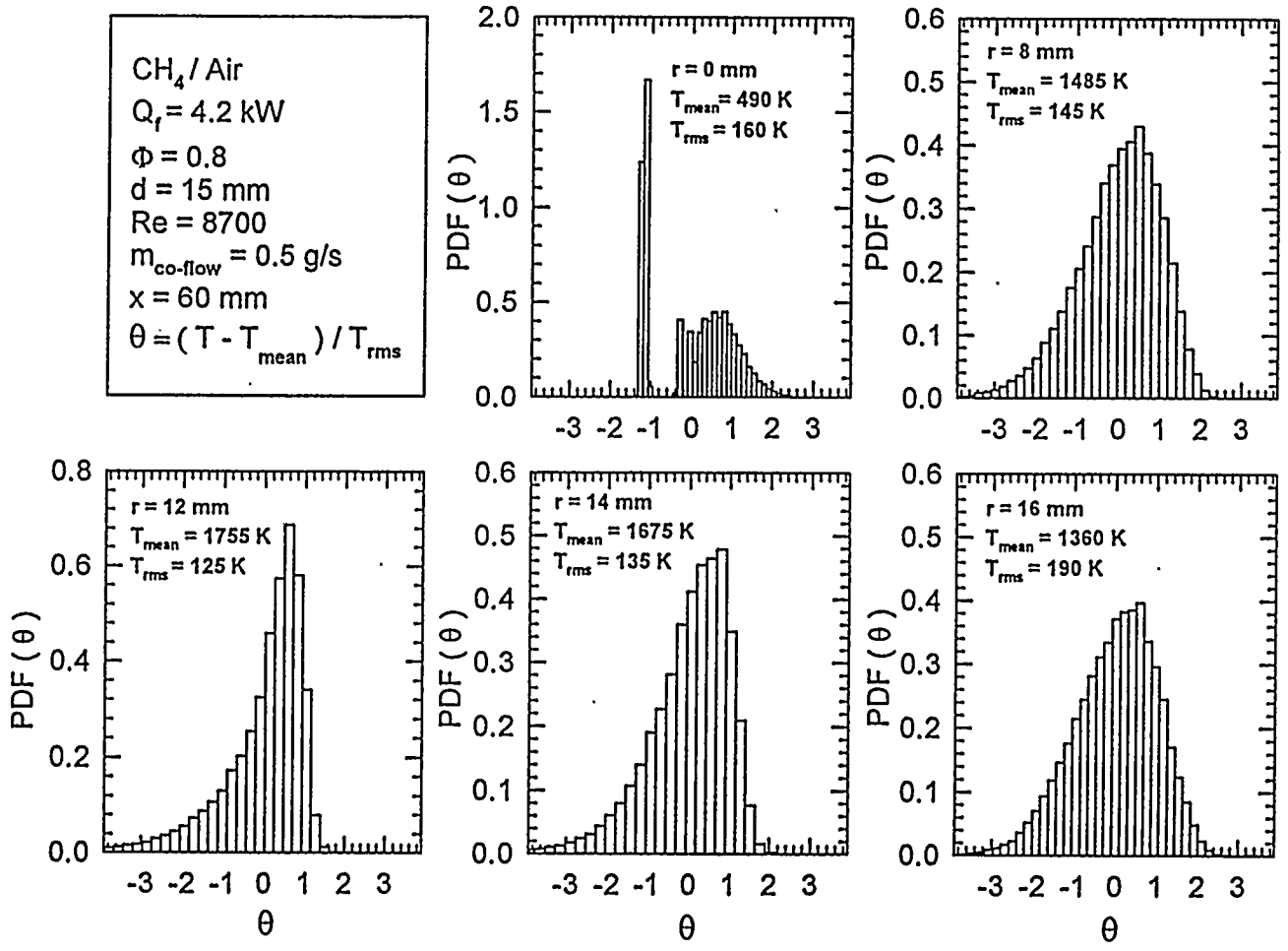

Figure 6. Probability Density Functions of Temperatures Measured in a Lean Premixed Flame

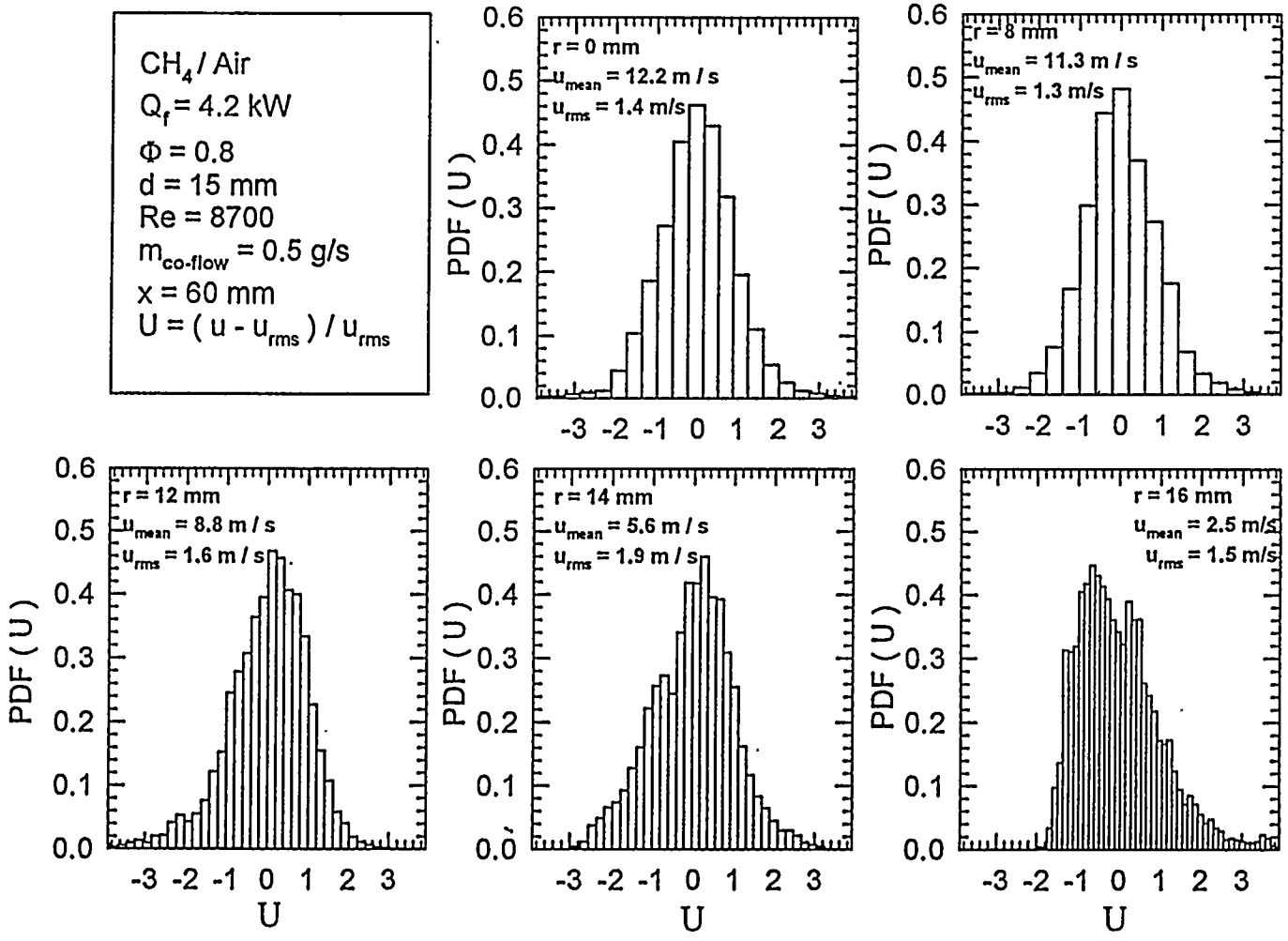

Figure 7. Probability Density Functions of Velocities Measured in a Lean Premixed Flame

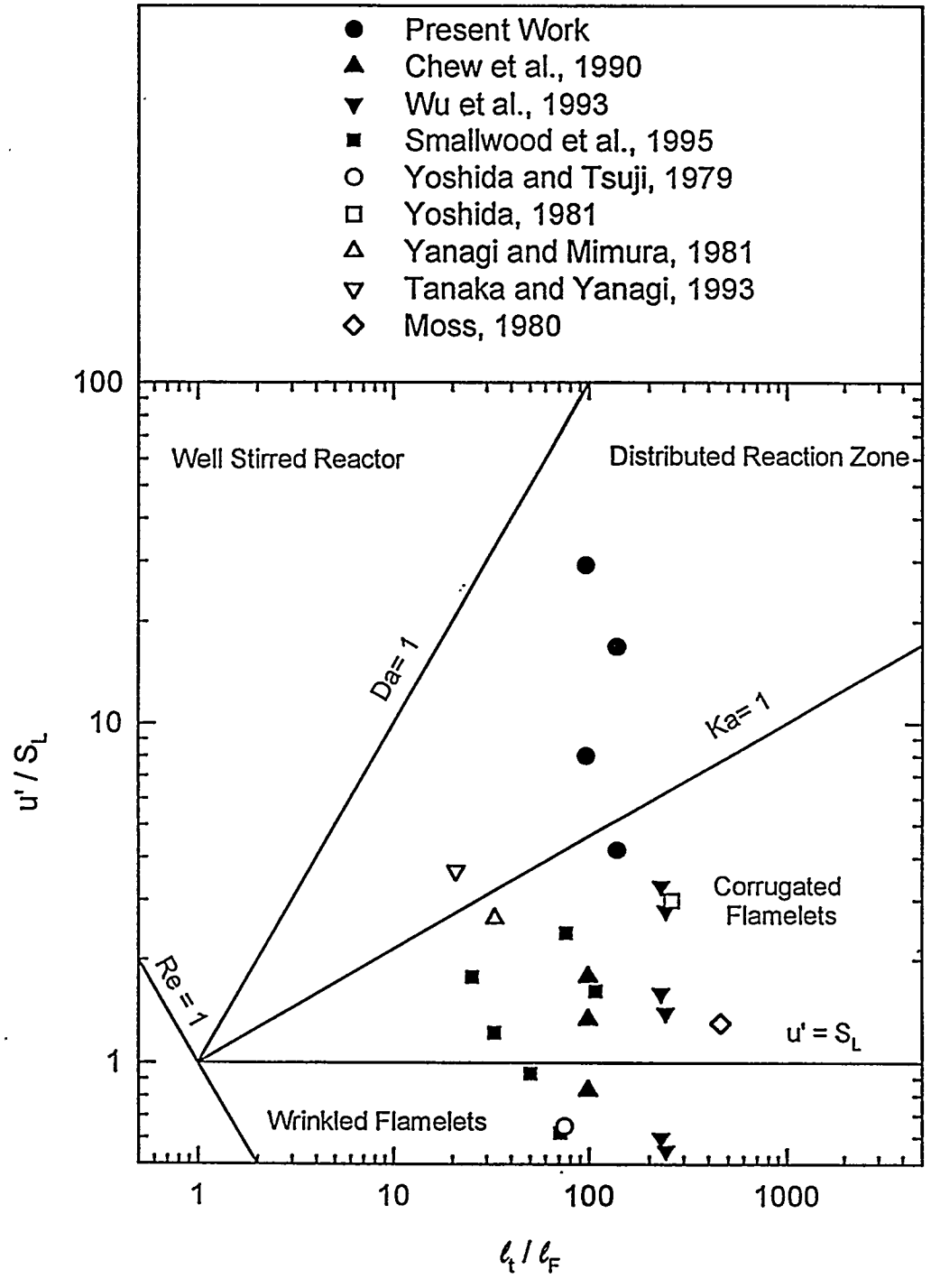

Figure 8. Phase Diagrams for Premixed Turbulent Flames

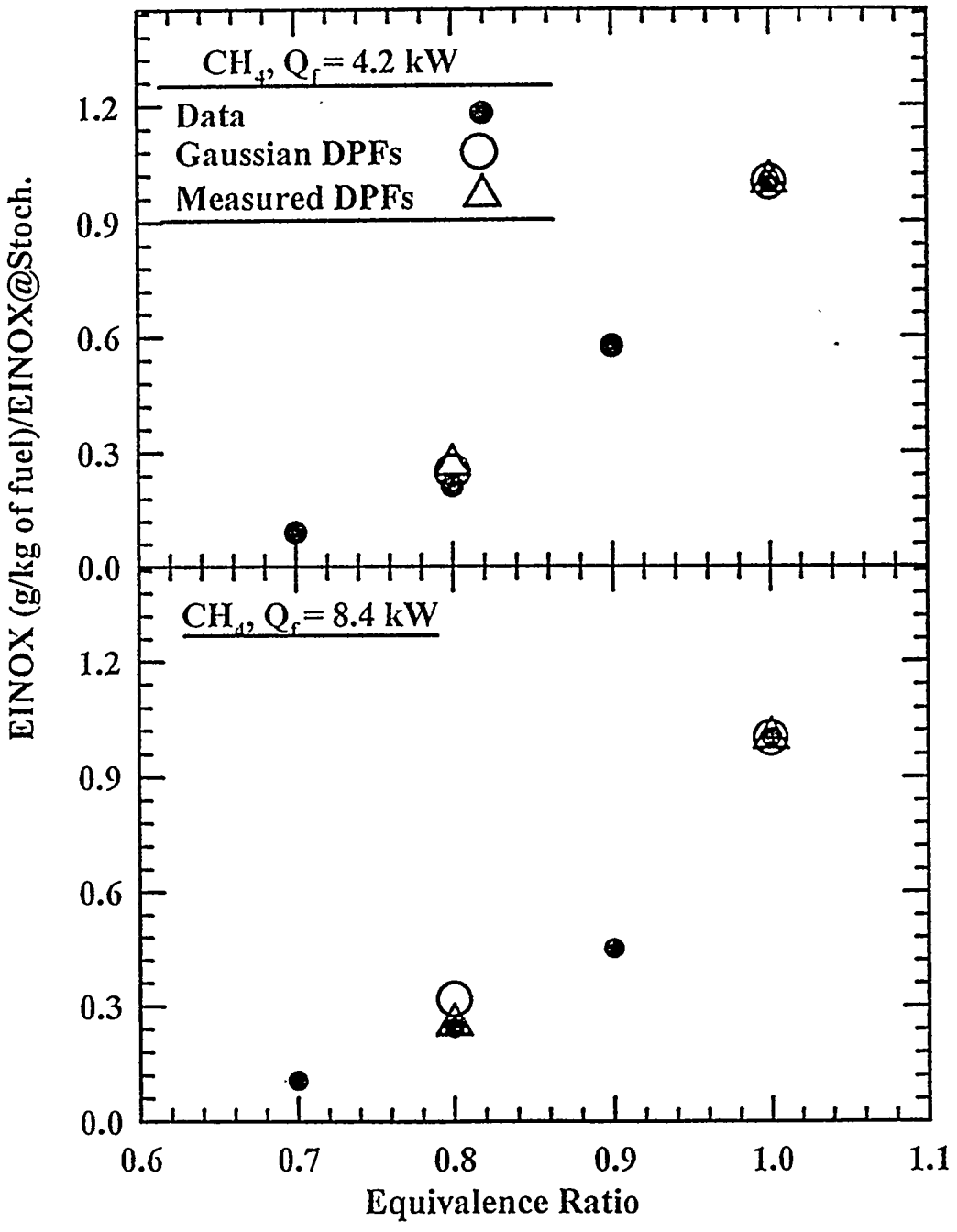

Figure 9. Measurements and Predictions of $EINO_x$ for the Premixed Turbulent Flames

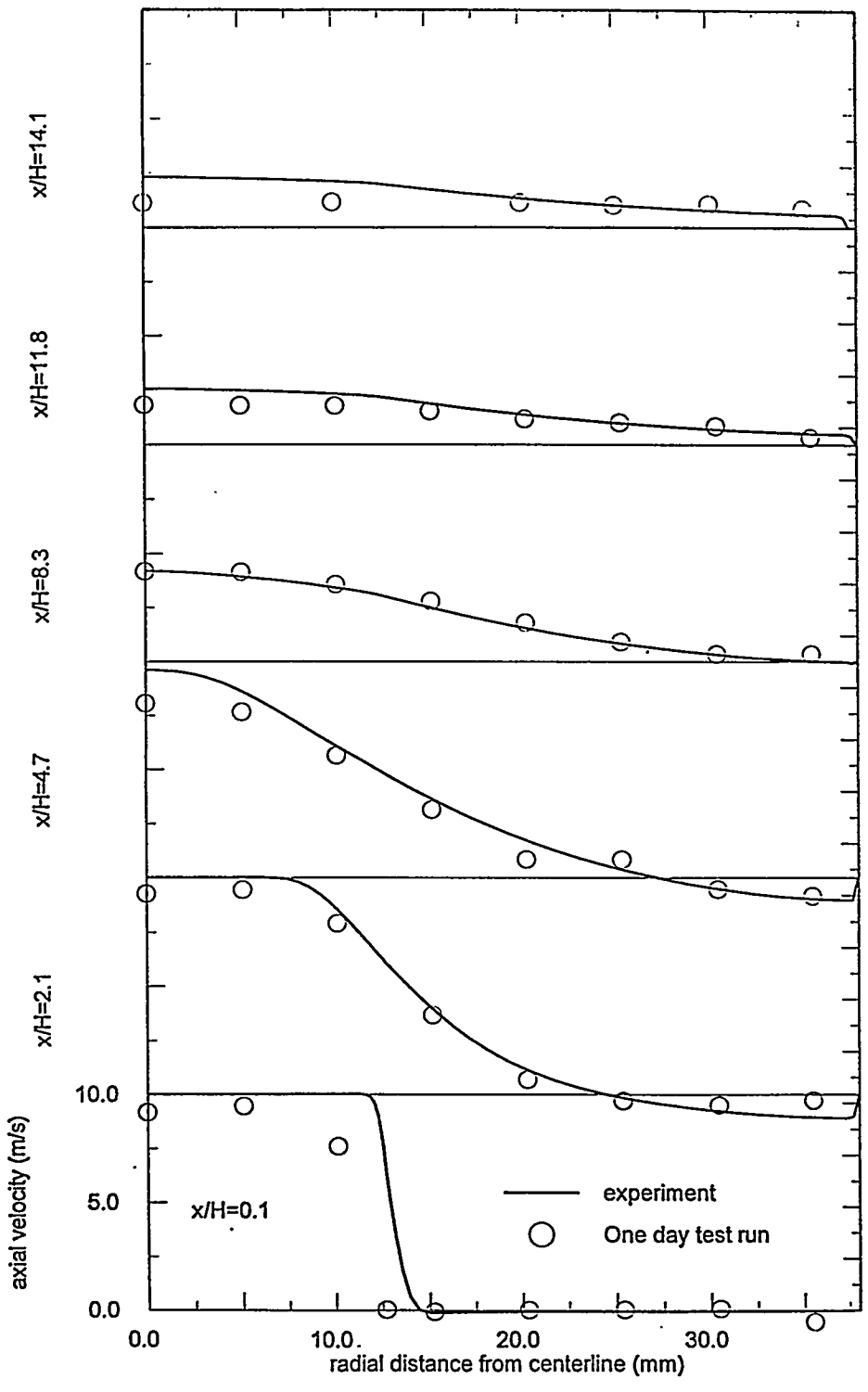

Figure 12. Axial Velocity Versus Radial Position at Six Axial Locations for the Combustor Operating at 10 atm and an Inlet Temperature of 450 K

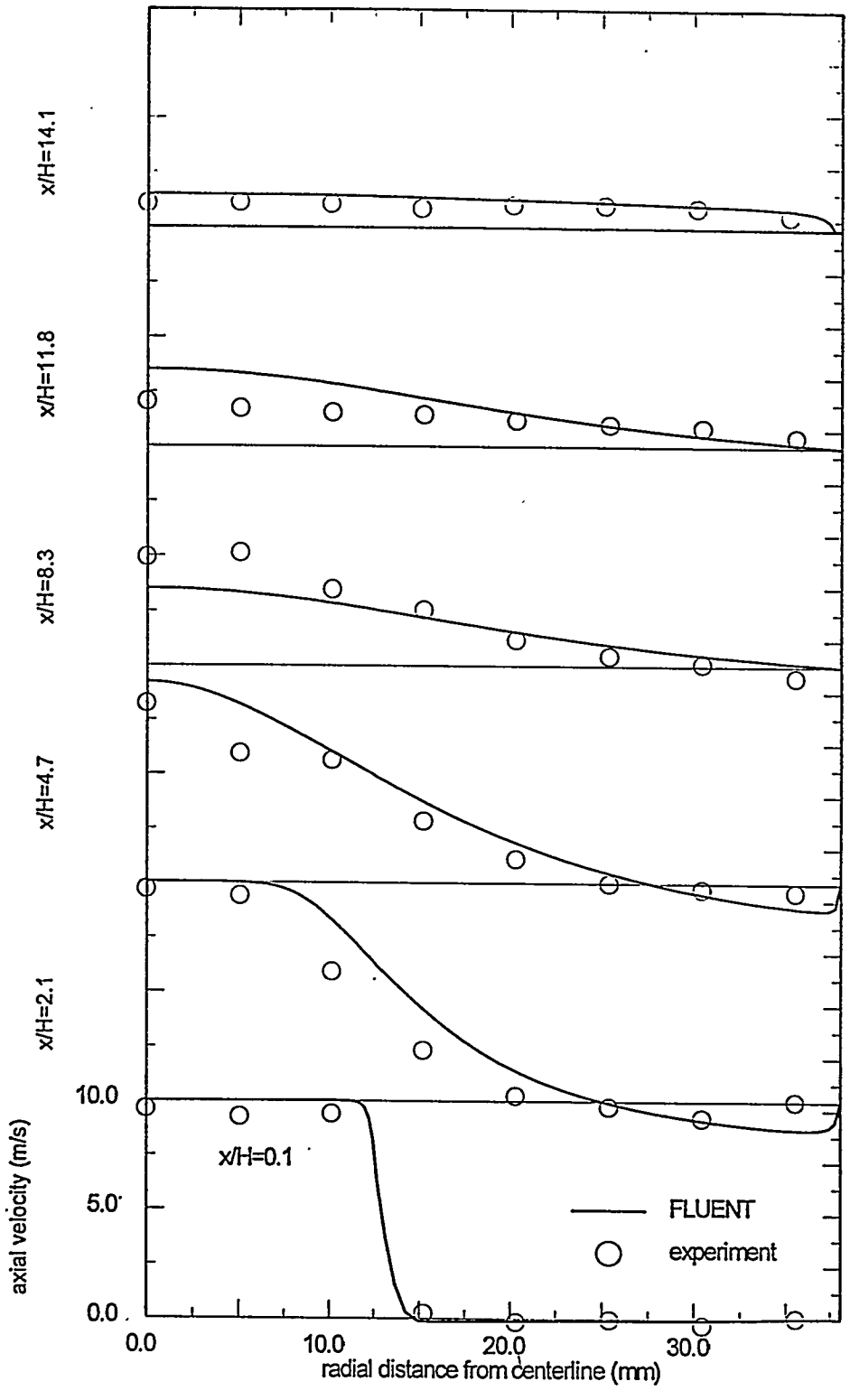

Figure 10. Axial Velocity Versus Radial Position at Six Axial Locations for the Combustor Operating at 2 atm and an Inlet Temperature of 383 K

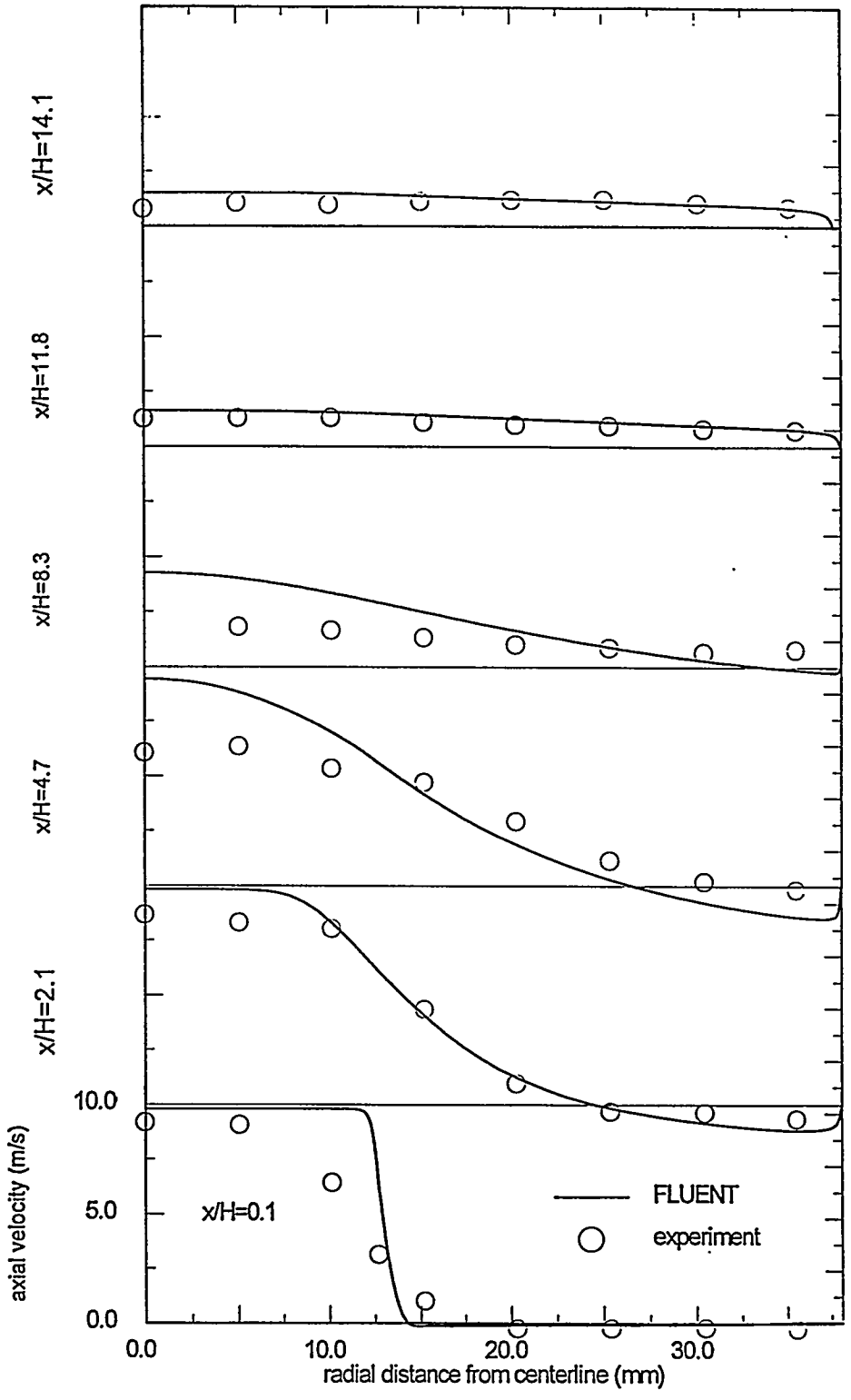

Figure 11. Axial Velocity Versus Radial Position at Six Axial Locations for the Combustor Operating at 5 atm and an Inlet Temperature of 439 K

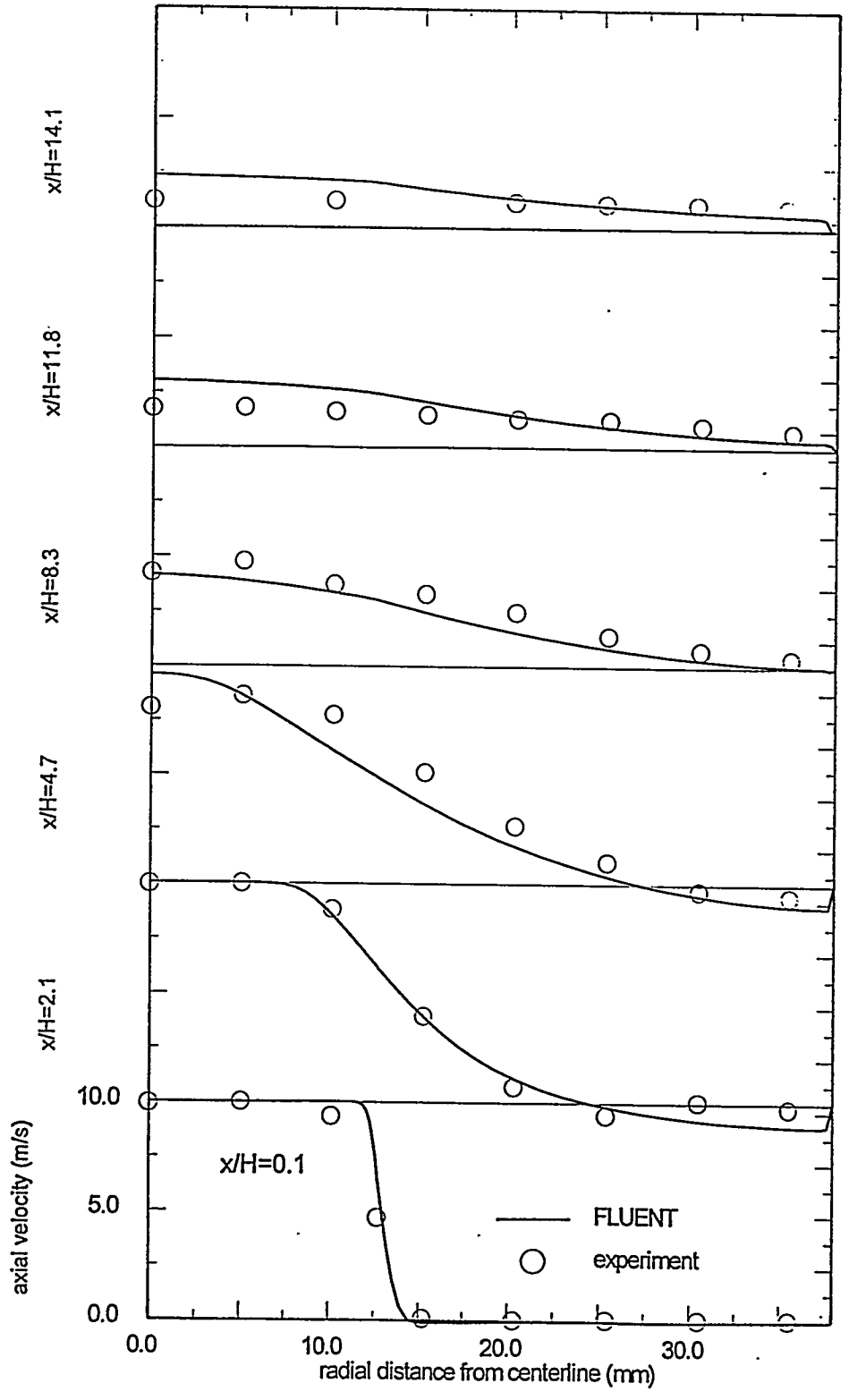

Figure 13. Axial Velocity Versus Radial Position at Six Axial Locations for the Combustor Operating at 15 atm and an Inlet Temperature of 477 K